Available online at www.sciencedirect.com
ScienceDirect
Journal of Sound and Vibration 323 (2009) 989–1002
JOURNAL OF SOUND AND VIBRATION
www.elsevier.com/locate/jsvi

Acoustic radiation from cylindrical transducer arrays

P.A. Nishamol, Jasmine Mathew, D.D. Ebenezer*

Naval Physical and Oceanographic Laboratory, Thrikkakara, Kochi 682021, India

Received 31 May 2008; received in revised form 8 November 2008; accepted 9 January 2009
Handling Editor: L.G. Tham
Available online 25 February 2009

Abstract

A method is presented to determine the omni-directional and directional far-field pressures radiated by cylindrical transducer arrays in an infinite rigid cylindrical baffle. The solution to the Helmholtz equation and the displacement continuity condition at the interface between the array and the surrounding water are used to determine the pressure. The displacement of the surface of each piston transducer is in the direction of the normal to the array and is assumed to be uniform. Expressions are derived for the pressure radiated by a sector of the array vibrating in-phase, the entire array vibrating in-phase, and a sector of the array phase-shaded to simulate radiation from a rectangular piston. It is shown that the uniform displacement required for generating a source level of 220 dB ref. μPa at 1 m that is omni-directional in the azimuthal plane is in the order of 1 μm for typical arrays. Numerical results are presented to show that there is only a small difference between the on-axis pressures radiated by phased cylindrical arrays and planar arrays.

1. Introduction

Cylindrical arrays of underwater electroacoustic transducers [1] can be used to radiate acoustic pressure that is omni-directional in the azimuthal plane or appears to emanate from a planar array. In this paper, an analytical method is presented to determine the omni-directional far-field pressure radiated by a full array of pistons and the directional far-field pressure radiated by a sector of the array.

Methods used to study acoustic radiation from underwater structures can be extended to study arrays. Analytical methods have been used to study forced vibrations of fluid-loaded cylindrical shells. In the first step, the displacement on the surface is specified and used to determine the self and mutual radiation impedances [2,3]. In the second step, the force on the structure is specified and the non-uniform displacement of the fluid-loaded structure is determined by using the radiation impedances which embody all the effects of the fluid [4,5]. Then, in the third step, the displacement is used to determine the far-field pressure [6].

The three-step approach can be extended, as follows, to develop an analytical model of a cylindrical array of transducers. The transducers are electrically driven by applying voltage. The displacement on the face of each transducer is approximately uniform because the face of the transducer is small with respect to a wavelength in water but depends, unless controlled, on the location of the transducer in the array. Therefore, in the first step,

*Corresponding author. Fax: +91 484 242 4858.
E-mail addresses: tsonpol@vsnl.com, d.d.ebenezer@gmail.com (D.D. Ebenezer).

0022-460X/$ - see front matter © 2009 Elsevier Ltd. All rights reserved.
doi:10.1016/j.jsv.2009.01.026

the self and mutual radiation impedances of pistons in an infinite rigid cylindrical baffle [7,8] are determined. In the second step, the displacements of the radiating faces of the fluid-loaded transducers in response to the electrical excitation are determined by using the radiation impedances that embody all the effects of the surrounding water. The far-field radiated pressure due to the non-uniform displacement is of final interest and is determined in the third step.

Alternatively, numerical methods can be used to simultaneously solve the governing equations in the water and the transducers but these are not without difficulties. Lam [9] analyzed an array of Tonpilz transducers. Benthien [10] presented model and experimental results for a linear array of three flextensional transducers. He showed that the center transducer will "take in" power at some frequencies—where the radiation resistance is negative.

It is not necessary to model the transducer if it is assumed that the displacement of each transducer is known. This assumption was made by Laird and Cohen [11] who studied radiation from one piston source in an infinite rigid cylindrical baffle, Rolleigh et al. [12] who compared the theoretical vertical beam pattern radiated by a cylindrical array with experimental results and suggested a method to suppress vertical side-lobes, and by Ebenezer [13] who studied directional radiation from a sparse array of piston transducers used for underwater communication and obtained good agreement with experimental results. This assumption can be dropped if the displacement of each piston is calculated using steps one and two described above.

In this paper, a method is presented to determine the pressure radiated by a cylindrical array of piston transducers with uniform displacement on the face of each transducer. It is assumed that the array is in an infinite, rigid, cylindrical baffle. In the present analysis, all the pistons in the same column or stave vibrate in-phase but the more general case of each piston vibrating with a different displacement can also be analyzed using the same method. First, an analysis of the pressure radiated by adjacent staves vibrating in-phase is presented primarily to introduce various definitions, sign conventions, and assumptions used later in the phased-array analysis. This analysis was first presented by Laird and Cohen [11] and used by Rolleigh et al. [12]. Then, the effect of phase shading on the maximum pressure and the beamwidth are presented. Phase shading is used in directional transmission [14] to increase the on-axis pressure. The method of stationary phase is used to determine the far-field pressure and numerical results are presented to illustrate the applications.

2. Theory

Consider a cylindrical array of electroacoustic piston transducers as shown in Fig. 1. The radius of the array is a. There are M transducers in the circumferential direction and each subtends an angle $2\pi/M$ at the center.

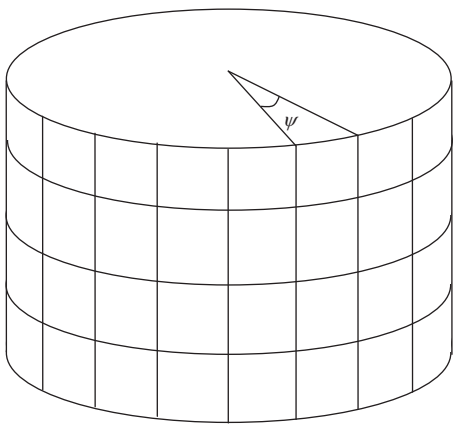

Fig. 1. Schematic of a cylindrical array of transducers. Each square on the curved surface of the cylinder represents the radiating face of one transducer. The radius and length of the array are a and $2L$, respectively. There are M transducers in the circumferential direction. $\psi = 2\pi/M$ is the angle subtended by each stave at the center. Each stave has N transducers in the vertical direction. It is assumed that the array is in an infinite, rigid, cylindrical baffle that is not shown.

The height of the array is $2L$ and there are N transducers in the vertical direction. It is assumed that the array is in an infinite, rigid, cylindrical baffle. The density and speed of sound in the surrounding water are ρ and c, respectively.

2.1. In-phase radiation from transducers

Consider first the case where $J \leqslant M$ adjacent staves vibrate uniformly with the same displacement and in-phase. Each stave consists of N transducers in the vertical direction. The surface of the rigid baffle does not vibrate even though the vibration of the transducers causes acoustic waves in the surrounding water. Therefore, the radial component of displacement on the surface of the cylinder is expressed in the cylindrical co-ordinates (r, ϕ, z) shown in Fig. 2 as

$$U(r,\phi,z) = \begin{cases} U_0; & |z| \leqslant L;\ \ r = a;\ |\phi| \leqslant \phi_0, \\ 0 & \text{otherwise}, \end{cases} \tag{1}$$

where U_0 is the amplitude and $\phi_0 = \pi J/M$. The term $e^{-j\omega t}$ where t denotes time and ω is the angular frequency is suppressed in all the equations for convenience.

The radial component of displacement on the surface of the transducers and the baffle is equal to the radial component of displacement in the water at $r = a$ for all z. This continuity condition is used to determine coefficients in the solution to the Helmholtz wave equation that governs acoustic waves in fluids. The continuity condition can be satisfied at a large but finite number of points with various values of z on $r = a$. Alternatively, it can be satisfied in wavenumber—frequency space. The radial component of displacement is discontinuous at $|z| = L$ because only the transducers vibrate and the baffle is rigid. Therefore, the second approach is used here.

A spatial Fourier transform pair is defined as

$$\hat{H}(k_z) = \int_{-\infty}^{\infty} H(z)\, e^{jk_z z}\, dz,$$
$$H(z) = \frac{1}{2\pi}\int_{-\infty}^{\infty} \hat{H}(k_z)\, e^{-jk_z z}\, dk_z, \tag{2}$$

where k_z is the wavenumber. Then, transforming Eq. (1) in the axial direction and expanding it using Fourier series in the ϕ direction yields

$$\hat{U}(r,\phi,k_z) = 2U_0 \frac{\sin(k_z L)}{k_z} \sum_{n=0}^{\infty} a_n \cos(n\phi), \tag{3a}$$

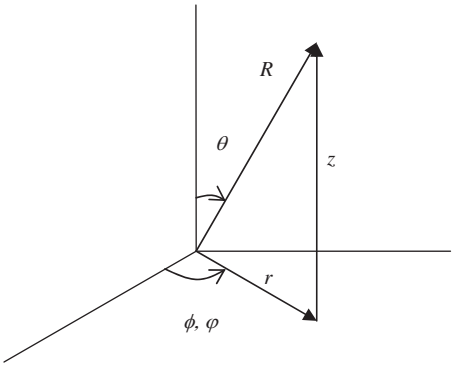

Fig. 2. The cylindrical coordinate system (r, ϕ, z) and the spherical coordinate system (R, θ, φ) used in the analysis.

where

$$a_n = \begin{cases} \phi_0/\pi; & n = 0, \\ 2\sin(n\phi_0)/(n\pi); & n = 1, 2, \ldots . \end{cases} \tag{3b}$$

The solution to the Helmholtz wave equation, in cylindrical coordinates, is expressed in wavenumber—frequency space as

$$\hat{P}(r, \phi, k_z) = \sum_{n=0}^{\infty} P_n(k_z) L_n(\beta r) \cos(n\phi), \tag{4a}$$

where

$$L_n(\beta r) = \begin{cases} H_n^{(1)}(\beta r); & \beta \text{ real and positive, } k > 0, \\ H_n^{(2)}(\beta r); & \beta \text{ real and negative, } k > 0, \\ K_n(\eta r); & \eta^2 = -\beta^2, \ \beta \text{ imaginary}, \end{cases} \tag{4b}$$

where P denotes pressure, $\beta = (k^2 - k_z^2)^{0.5}$, $k = \omega/c$ is the angular wavenumber, $H_n^{(i)}(.)$ is the nth order Hankel function of the ith kind, and $K_n(.)$ is the nth order modified Bessel function of the second kind. It is noted that the solution satisfies the Sommerfield radiation condition [15].

The radial displacement on the surface of the array is equal to the radial displacement in the water. It, therefore, follows that

$$\hat{U}(r, \phi, k_z) = \frac{-1}{\rho\omega^2} \frac{\partial \hat{P}(r, \phi, k_z)}{\partial r}, \tag{5}$$

where the convention that extensional pressure is positive is used. Substituting Eqs. (3) and (4) in Eq. (5) yields

$$P_n(k_z) = -2\rho\omega^2 U_0 \frac{\sin(k_z L)}{k_z} \frac{a_n}{\beta L_n'(\beta a)}. \tag{6}$$

The pressure is then determined by substituting Eq. (6) in Eq. (4a) and evaluating the inverse Fourier transform:

$$P(r, \phi, z) = \frac{-\rho\omega^2 U_0}{\pi} \int_{-\infty}^{\infty} \frac{\sin(k_z L)}{k_z} \sum_{n=0}^{\infty} \frac{L_n(\beta r)}{\beta L_n'(\beta a)} a_n \cos(n\phi) \, \mathrm{e}^{-\mathrm{j}k_z z} \, \mathrm{d}k_z, \tag{7}$$

where prime denotes derivative with respect to the argument.

$P(r, \phi, z)$ should be an even function of z when U is an even function of z. This is seen to be the case when $\hat{P}(r, \phi, k_z)$ is an even function of k_z. Therefore, it is assumed that β is real and positive when $|k_z| < k$. It then follows from Eqs. (7) and (4) that

$$\begin{aligned} P(r, \phi, z) = \frac{-\rho\omega^2 U_0}{\pi} X \Bigg\{ & \int_{-\infty}^{-k} \frac{\sin(k_z L)}{k_z} \sum_{n=0}^{\infty} \frac{K_n(\eta r)}{\eta K_n'(\eta a)} a_n \cos(n\phi) \, \mathrm{e}^{-\mathrm{j}k_z z} \, \mathrm{d}k_z \\ & + \int_{-k}^{k} \frac{\sin(k_z L)}{k_z} \sum_{n=0}^{\infty} \frac{H_n^{(1)}(\beta r)}{\beta H_n^{(1)'}(\beta a)} a_n \cos(n\phi) \, \mathrm{e}^{-\mathrm{j}k_z z} \, \mathrm{d}k_z \\ & + \int_{k}^{\infty} \frac{\sin(k_z L)}{k_z} \sum_{n=0}^{\infty} \frac{K_n(\eta r)}{\eta K_n'(\eta a)} a_n \cos(n\phi) \, \mathrm{e}^{-\mathrm{j}k_z z} \, \mathrm{d}k_z \Bigg\}. \end{aligned} \tag{8}$$

The pressure in the far field is of primary interest. Using the large argument approximation for $K_n(\eta r)$ and $H_n^{(1)}(\beta r)$ yields

$$P(r,\phi,z)=\frac{-\rho\omega^2}{\pi}U_0\sum_{n=0}^{\infty}a_n\cos(n\phi)X\left\{\left(\frac{\pi}{2r}\right)^{0.5}\int_{-\infty}^{-k}\frac{\sin(k_zL)}{k_z}\frac{\mathrm{e}^{-\eta r}}{\eta^{1.5}K_n'(\eta a)}\mathrm{e}^{-\mathrm{j}k_zz}\,\mathrm{d}k_z+\left(\frac{2}{\pi r}\right)^{0.5}\int_{-k}^{k}\frac{\sin(k_zL)}{k_z}\frac{\mathrm{e}^{\mathrm{j}(\beta r-k_zz)}}{\beta^{1.5}H_n^{(1)'}(\beta a)}\mathrm{e}^{-\mathrm{j}(2n+1)\pi/4}\,\mathrm{d}k_z+\left(\frac{\pi}{2r}\right)^{0.5}\int_{-k}^{\infty}\frac{\sin(k_zL)}{k_z}\frac{\mathrm{e}^{-\eta r}}{\eta^{1.5}K_n'(\eta a)}\mathrm{e}^{-\mathrm{j}k_zr}\,\mathrm{d}k_z\right\}. \tag{9}$$

In the far field, r is very large and the first and third integrals in Eq. (9) are neglected because they contain exponentially decaying terms. The expression for pressure then reduces to

$$P(r,\phi,z)=\frac{-\rho\omega^2}{\pi}U_0\left(\frac{2}{\pi r}\right)^{0.5}\sum_{n=0}^{\infty}a_n\mathrm{e}^{-\mathrm{j}(2n+1)(\pi/4)}\cos(n\phi)\int_{-k}^{k}\Gamma_n(r,\phi,z,k_z)\,\mathrm{d}k_z, \tag{10a}$$

where

$$\Gamma_n(r,\phi,z,k_z)=\frac{\sin(k_zL)}{k_z}\frac{\mathrm{e}^{\mathrm{j}(\beta r-k_zz)}}{\beta^{1.5}H_n^{(1)'}(\beta a)} \tag{10b}$$

and is evaluated by using the method of stationary phase. The primary contribution to the integral comes from $k_z=kz/\sqrt{r^2+z^2}$ and the approximation made by neglecting the first and third integrals in Eq. (9) is, therefore, justified. Finally, the pressure in the far field is expressed as

$$P(r,\phi,z)=\frac{\mathrm{j}2\rho\omega^2U_0}{\pi}\frac{\sin\left(\frac{kzL}{\sqrt{r^2+z^2}}\right)}{\left(\frac{kz}{\sqrt{r^2+z^2}}\right)}\frac{\mathrm{e}^{\mathrm{j}k((r^2-z^2)/(\sqrt{r^2+z^2}))}}{kr}\sum_{n=0}^{\infty}\frac{a_n\mathrm{e}^{-\mathrm{j}n\pi/2}}{H_n^{(1)'}\left(\frac{kra}{\sqrt{r^2+z^2}}\right)}\cos(n\phi). \tag{11}$$

The pressure in the plane midway between the ends of the cylindrical array ($z=0$) is of primary interest. In this plane, the above expression reduces to [11]

$$P(r,\phi,z=0)=\frac{\mathrm{j}2\rho cL\omega U_0}{\pi r}\mathrm{e}^{\mathrm{j}kr}\sum_{n=0}^{\infty}a_n\frac{\mathrm{e}^{-\mathrm{j}n\pi/2}}{H_n^{(1)'}(ka)}\cos(n\phi). \tag{12}$$

Consider now the special case where all the transducer staves are vibrating in-phase, i.e. $J=M$ and $\phi_0=\pi$. This corresponds to omni-directional radiation in the azimuthal plane from the array. Substituting $a_n=0$ for $n=1,2,\ldots$ for this case and $\varphi=0$ in Eq. (12) to determine the pressure in the direction of the normal to the surface of cylinder yields

$$P(r,\phi=0,z=0)=\frac{\mathrm{j}2\rho cL\omega U_0}{\pi r}\frac{\mathrm{e}^{\mathrm{j}kr}}{H_0^{(1)'}(ka)}. \tag{13}$$

When ka is small, Eq. (13) reduces to

$$P(r,\phi=0,z=0)=\rho A_0S\frac{\mathrm{e}^{\mathrm{j}kr}}{4\pi r}, \tag{14a}$$

where $A_0 = -\omega^2 U_0$ is the acceleration on the surface and S is the surface area of the radiator. The expressions for far-field pressure on the axis of circular and rectangular pistons:

$$P(R, \pi/2, \varphi) = \rho A_0 S \frac{e^{jkR}}{2\pi R} \tag{14b}$$

and spheres

$$P(R, \pi/2, \varphi) = \rho A_0 S \frac{e^{jkR}}{4\pi R} \tag{14c}$$

are similar. $S = 4\pi aL$ in Eq. (14a) and $4\pi b^2$ in Eq. (14c) where b is the radius of the sphere. It is noted that the radiated pressure, at low frequencies, is independent of frequency and proportional to the uniform acceleration and surface area.

When ka is large, as is usually the case in arrays, Eq. (13) reduces to

$$P(r, \phi = 0, z = 0) = (1 + j)\sqrt{\frac{ac}{\pi}} \frac{\rho L \omega^{3/2} U_0}{r} e^{jkr}. \tag{15}$$

Eq. (15) shows that there is a 9 dB increase per octave in the radiated pressure when the displacement on the surface of the cylinder is independent of frequency. However, in transducers, the displacement on the surface will increase when the frequency is less than the resonance frequency of the transducer and decrease after reaching a maximum. Therefore, Eq. (15) shows that the bandwidth of the transducer is increased in the upper sideband by the increase in the radiation efficiency of the cylindrical array.

2.2. Phased radiation from transducers in a sector

Consider now the case where the amplitude and phase of vibration of each stave is independently controlled but the displacement is uniform on the surface of each stave. This is done to simulate radiation from a rectangular array or generate a beam pattern with a desired shape in the azimuthal direction.

When J staves vibrate, the displacement on the surface of the cylinder is

$$U(a, \phi, z) = \sum_{m=1}^{J} U_m(a, \phi, z), \tag{16a}$$

where

$$U_m(a, \phi, z) = \begin{cases} A_m; & |\phi - \phi_m| \leqslant \phi_0; \ \ |z| \leqslant L, \\ 0 & \text{otherwise} \end{cases} \tag{16b}$$

is the displacement of the mth stave, A_m is complex and is used to control the amplitude and phase, ϕ_m is the center of the mth stave, and $\phi_0 = \pi/M$.

Expanding the displacement in a Fourier series in the ϕ-direction and using the Fourier transform in Eq. (2) yields

$$\hat{U}(a, \phi, k_z) = \sum_{m=1}^{J} \hat{U}_m(a, \phi, k_z), \tag{17a}$$

where

$$\hat{U}_m(a, \phi, k_z) = 2A_m(\omega) \frac{\sin(k_z L)}{k_z} \sum_{n=0}^{\infty} [B_{mn} \cos(n\phi) + C_{mn} \sin(n\phi)], \tag{17b}$$

$$B_{mn} = \begin{cases} \dfrac{\phi_0}{\pi}; & n = 0, \\ \dfrac{2}{n\pi}\cos(n\phi_m)\,\sin(n\phi_0); & n = 1, 2, \ldots \end{cases} \tag{17c}$$

and

$$C_{mn} = \begin{cases} 0; & n = 0, \\ \dfrac{2}{n\pi}\sin(n\phi_m)\,\sin(n\phi_0); & n = 1, 2, \ldots . \end{cases} \tag{17d}$$

The appropriate form of the solution to the Helmholtz wave equation, in cylindrical coordinates and wavenumber space is

$$\hat{P}(r, \phi, k_z) = \sum_{n=0}^{\infty}[P_n\,\cos(n\phi) + Q_n\,\sin(n\phi)]L_n(\beta r). \tag{18}$$

The coefficients P_n and Q_n are determined by using the displacement continuity condition at the interface between the cylinder and water in Eq. (5). Then, using Eq. (2) to determine the inverse Fourier transform of (18) yields

$$P(r, \phi, z) = \frac{-\rho\omega^2}{\pi}\int_{-\infty}^{\infty}\frac{\sin(k_z L)}{k_z}\sum_{n=0}^{\infty}\frac{L_n(\beta r)}{\beta L_n'(\beta a)}\sum_{m=1}^{J}A_m(\omega)[B_{mn}\,\cos(n\phi) + C_{mn}\,\sin(n\phi)]\,\mathrm{e}^{-\mathrm{j}k_z z}\,\mathrm{d}k_z. \tag{19}$$

Now consider the case there the phase of each stave is controlled to simulate radiation from a rectangular array. A top view of the radiating sector of the cylindrical array is shown in Fig. 3 where the axis of the array passes through O. The J radiating staves are in the arc AB. Angle AOB is $2\pi J/M$. The center of the radiating sector is C and angle $AOC = \phi_c = \pi J/M$. Let D be the center of the mth stave. Then, angle $AOD = \phi_m = 2\pi(m - 0.5)/M$.

In order to simulate radiation from a rectangular array whose width is equal to the chord AB and height is $2L$, a phase delay that corresponds to the distance ED is applied to the mth stave. For convenience, an additional delay that corresponds to the distance OF is applied to all the J staves. Therefore, the total delay applied to the mth stave corresponds to $ED + OF = d_m = a\cos(\phi_m - \phi_c)$ and $A_m = U_0\,\mathrm{e}^{\mathrm{j}kd_m}$.

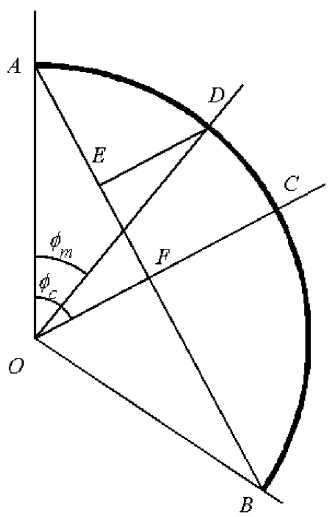

Fig. 3. Top view of the radiating sector of a cylindrical array. The transducers in the arc ACB radiate. Each stave is delayed by an appropriate amount to simulate radiation from the chord AB. The delay applied to the mth stave with center at D is ED. An additional delay OF is applied to all the staves. Therefore, the total delay is $a\cos(\phi_m - \phi_c)$.

Again, assuming that β is real and positive when $|k_z|<k$, and using the far-field approximation yields

$$P(r,\phi,z)=\frac{-\rho\omega^2}{\pi}U_0\sum_{m=1}^{J}e^{jkd_m}\sum_{n=0}^{\infty}[B_{mn}\cos(n\varphi)+C_{mn}\sin(n\varphi)]$$
$$\times\left\{\int_{-\infty}^{-k}\frac{\sin(k_zL)}{k_z}\left(\frac{\pi}{2\eta r}\right)^{1/2}\frac{e^{-\eta r}}{\eta K_n^{(1)'}(\eta a)}e^{-jk_zz}\,dk_z+\int_{-k}^{k}\frac{\sin(k_zL)}{k_z}\left(\frac{2}{\pi\beta r}\right)^{1/2}\frac{e^{j(\beta r-(2n+1)\pi/4)}}{\beta H_n^{(1)'}(\beta a)}e^{-jk_zz}\,dk_z\right.$$
$$\left.+\int_{-k}^{\infty}\frac{\sin(k_zL)}{k_z}\left(\frac{\pi}{2\eta r}\right)^{1/2}\frac{e^{-\eta r}}{\eta K_n^{(1)'}(\eta a)}e^{-jk_zz}\,dk_z\right\}. \tag{20}$$

Neglecting the first and third integrals in Eq. (20), using the method of stationary phase, and observing that the primary contribution to the second integral in Eq. (20) comes from $k_z=kz/(\sqrt{r^2+z^2})$ yields

$$P(r,\phi,z)=\frac{j2\rho\omega^2U_0}{\pi}\frac{e^{jk((r^2-z^2)/(\sqrt{r^2+z^2}))}}{kr}\frac{\sin\left(\dfrac{(kzL)}{\sqrt{r^2+z^2}}\right)}{\left(\dfrac{(kz)}{\sqrt{r^2+z^2}}\right)}$$
$$\times\sum_{n=0}^{\infty}\frac{e^{-jn\pi/2}}{H_n^{(1)'}\left(\dfrac{kra}{\sqrt{r^2+z^2}}\right)}\sum_{m=1}^{J}[B_{mn}\cos(n\varphi)+C_{mn}\sin(n\varphi)]e^{jkd_m}. \tag{21a}$$

In the plane midway between the ends of the cylindrical array ($z=0$) the pressure is expressed as

$$P(r,\phi,z=0)=\frac{j2\rho\omega cLU_0}{\pi r}e^{jkr}\sum_{n=0}^{\infty}\frac{e^{-jn\pi/2}}{H_n^{(1)'}(ka)}\sum_{m=1}^{J}[B_{mn}\cos(n\varphi)+C_{mn}\sin(n\varphi)]e^{jkd_m}. \tag{21b}$$

It is noted that the phased radiation only approximately simulates radiation from a rectangular piston because the vibration of each stave is in the radial direction and not in the direction along OC in Fig. 3.

The pressure [15] in the far field of a rectangular piston, vibrating with uniform displacement U_0, in an infinite rigid baffle is also evaluated using the method of stationary phase. It is expressed, in spherical coordinates (R,θ,φ) shown in Fig. 4, as

$$P_p(R,\theta,\varphi)=\frac{-2\rho\omega^2U_0}{\pi R}\frac{\sin(k\sin\theta\cos\varphi L_x)}{k\sin\theta\cos\varphi}\frac{\sin(k\sin\theta\sin\varphi L_y)}{k\sin\theta\sin\varphi}e^{jkR}, \tag{22}$$

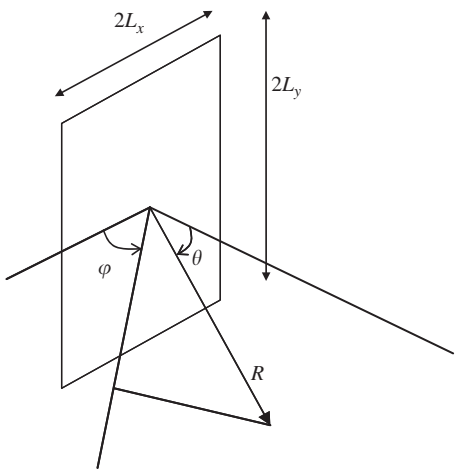

Fig. 4. Spherical coordinate system (R,θ,φ) for radiation from a rectangular piston of sides $2L_x$ and $2L_y$ [15]. $\theta=0$ along the axis of the piston.

where $2L_x$ is the width and $2L_y$ is the height of the rectangular piston. The pressure along the axis of the piston is determined by using $\theta = 0$ and reduces to Eq. (14b). The pressures radiated by the phased sector and the rectangular piston are compared in the next section.

3. Numerical results and discussions

Numerical results are presented for arrays *A* and *B*. Details of the arrays are presented in Table 1. The radii of the arrays are chosen to illustrate the effect of the normalized operating frequency on the radiated patterns. The speed of sound in water is $c = 1500\,\text{m/s}$ and the density of water is $\rho = 1000\,\text{kg/m}^3$. After checking for convergence, all numerical results obtained using Eq. (21b) have been computed by replacing the infinite sum by the sum of the first 25 terms.

The stationary phase method is used to evaluate the integrals. The function $\Gamma_n(r, \phi, z, k_z)$ in Eq. (10b) is shown in Fig. 5 to illustrate the rapid oscillations except near the stationary phase point: $k_z = 0$. The oscillations justify the assumption that the integral can be evaluated if the behavior of the function near the stationary phase point is known.

First, consider array *A*. The required source level (SL) of the array is specified to be 220 dB ref. μPa at 1 m in the omni-directional mode. It follows from Eq. (13) that the amplitude of displacement, U_0, is 0.996 μm. It is useful to note that the hydrostatic pressure due to a 10 m water column is about 10^5 Pa which is the acoustic pressure corresponding to 220 dB ref. μPa.

Consider, next, the case where only nine of the 30 staves vibrate with the displacement required to generate 220 dB in the omni-directional mode. The staves in the sector vibrate in-phase and the radiation is directional. It follows from Eq. (12) that the SL on the axis of the sector is 221.4 dB. The directivity pattern for this case is shown in Fig. 6a. The maximum does not occur on the axis of the sector but at $\pm 30^\circ$. When the number of

Table 1
Characteristics of arrays.

Array	Radius *a* (m)	Length 2*L* (m)	No. of staves	Operating frequency (kHz)	Normalised operating frequency *ka*
A [16]	0.365	0.635	30	10.5	16.1
B	0.4775	1	32	9, 7.5, 6	18, 15, 12

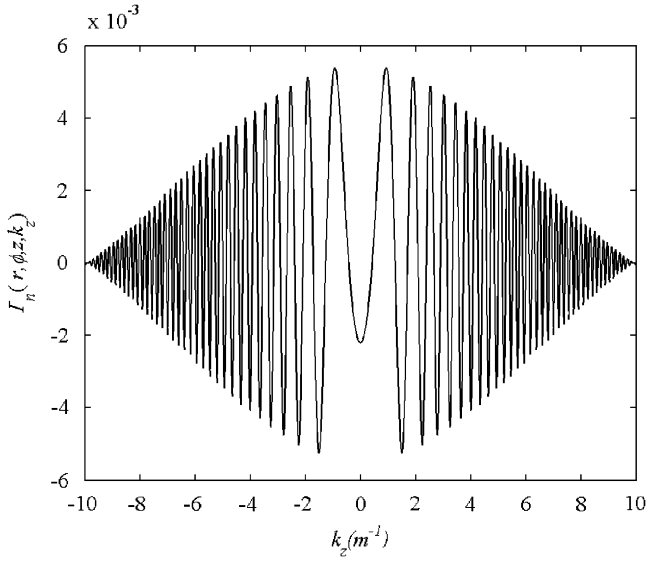

Fig. 5. The function Γ_n, in Eq. (10b), that is integrated using the method of stationary phase for array *A*, $f = 10.5\,\text{kHz}$, $n = 0$, $r = 200\,\text{m}$, $z = 0$, and $\varphi = 0$. There are rapid oscillations except near the stationary phase point: $k_z = 0$.

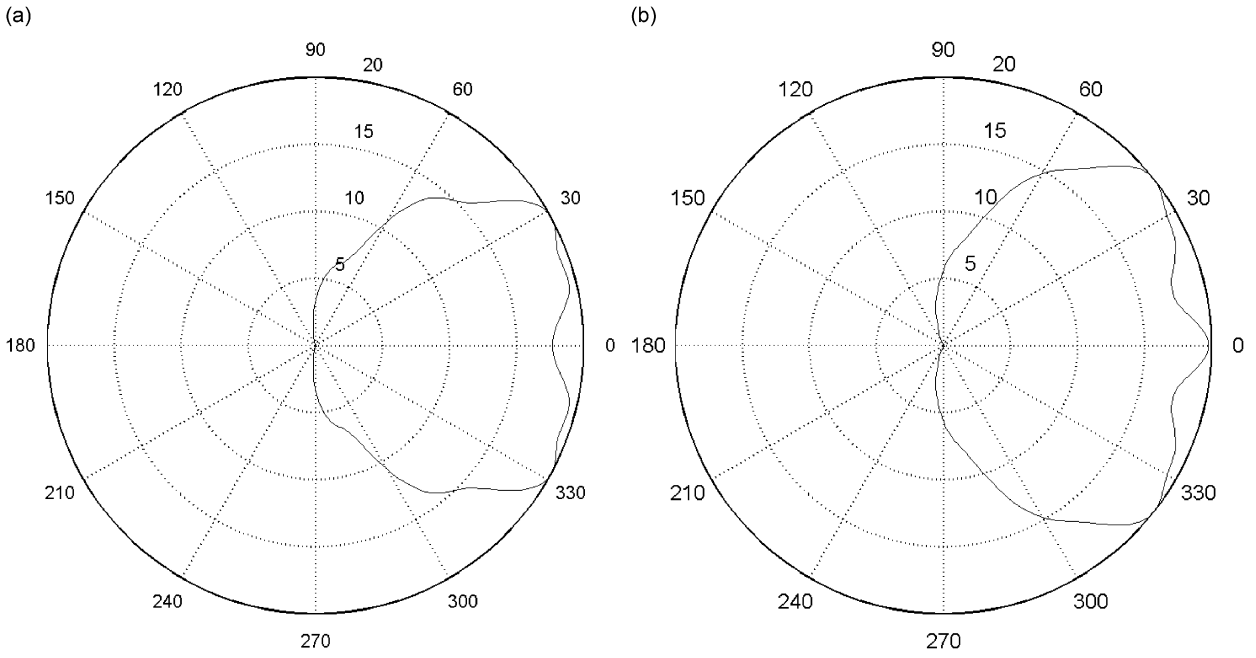

Fig. 6. Directivity patterns, in dB, due to in-phase vibration of (a) nine and (b) 11 staves out of 30 staves in array A at 10.5 kHz.

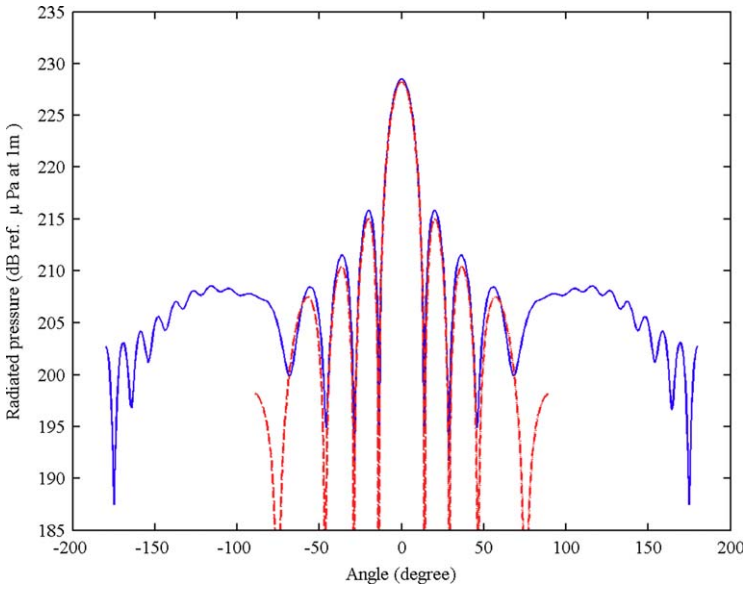

Fig. 7. Pressure radiated at 10.5 kHz by phased vibration of nine staves in array A (solid line) and a corresponding rectangular piston (dashed line).

staves is increased to 11, the maxima occur at 0° and at $\pm 40^\circ$ and the SL increases slightly to 221.5 dB as shown in Fig. 6b.

Consider, next, the case of phased radiation from nine of the 30 staves in array A. The delays are chosen to simulate radiation from a rectangular piston. The displacement amplitude is again 0.996 μm. The radiated pressure in the azimuthal plane is computed using Eq. (21b) and shown in Fig. 7 using a solid line. For comparison, the pressure radiated by a corresponding rectangular piston is computed using Eq. (22) and shown in Fig. 7 using a dashed line. The piston is mounted in an infinite rigid baffle and vibrates with the same

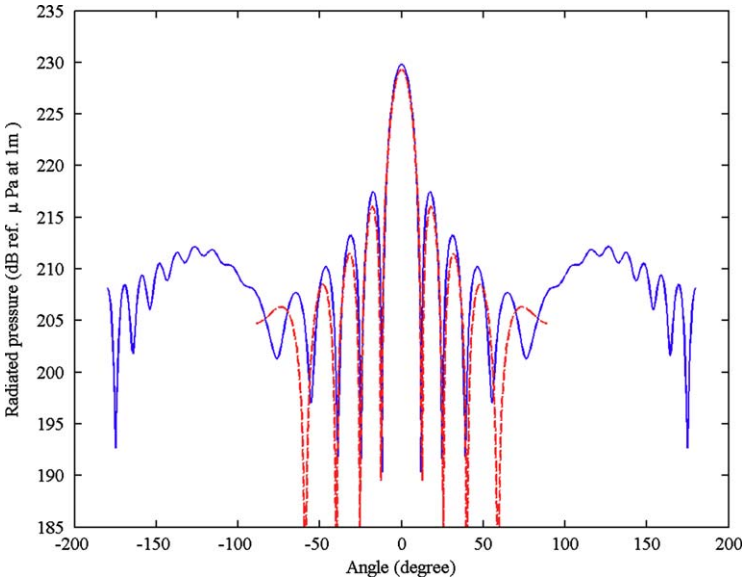

Fig. 8. Pressure radiated at 10.5 kHz by phased vibration of 11 staves in array *A* (solid line) and a corresponding rectangular piston (dashed line).

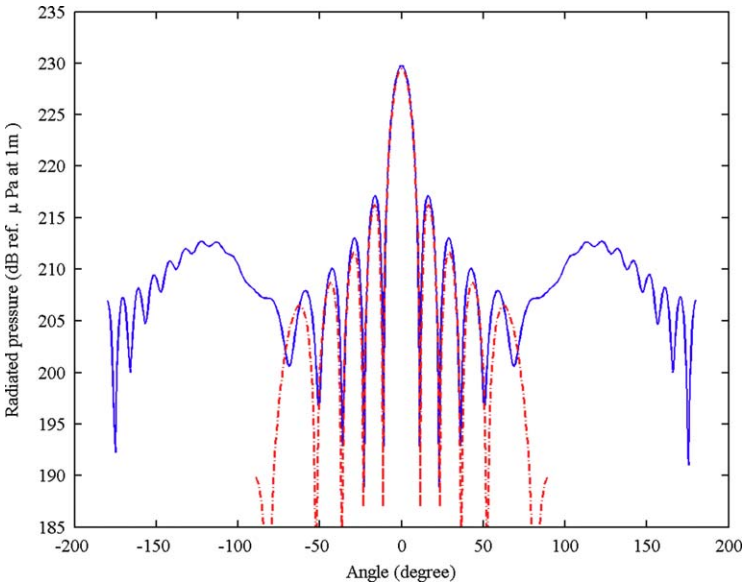

Fig. 9. Pressure radiated at 9 kHz by phased vibration of 11 staves in array *B* (solid line) and a corresponding rectangular piston (dashed line).

displacement. The length, 0.635 m, of the rectangular piston is equal to the length of the cylinder. Its width, 0.591 m, is equal to the length of the chord, *AB*, in Fig. 3. It is seen that the on-axis radiated pressure is 228.5 dB for the cylindrical sector and is a little more than the 228.2 dB radiated by the rectangular piston. The 3 dB beamwidths of the cylindrical sector and the piston are 12.15° and 12.3°, respectively. The main lobe of the cylindrical sector is a little wider and the side lobes are a little lesser than that of the piston. The piston does not radiate any energy behind the baffle but the sector radiates some energy in all directions.

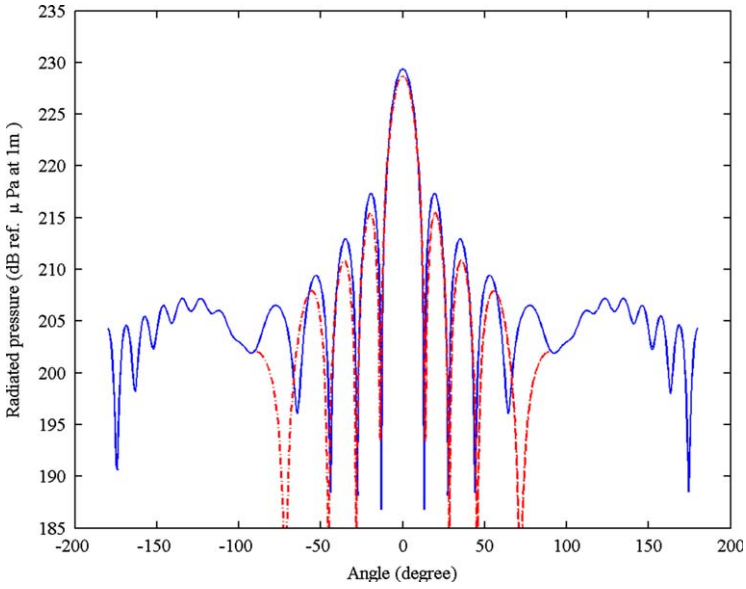

Fig. 10. Pressure radiated at 7.5 kHz by phased vibration of 11 staves in array *B* (solid line) and a corresponding rectangular piston (dashed line).

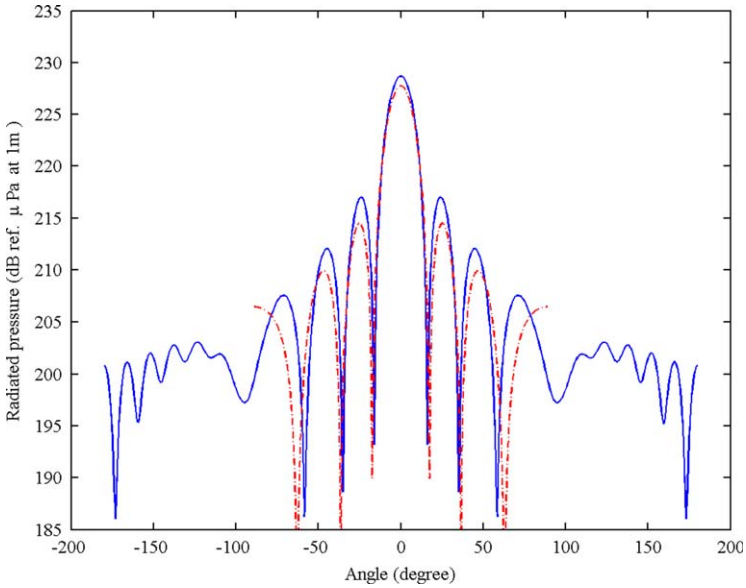

Fig. 11. Pressure radiated at 6 kHz by phased vibration of 11 staves in array *B* (solid line) and a corresponding rectangular piston (dashed line).

Phased radiation by 11 staves in array *A* is shown in Fig. 8. The pressure on the axis is 229.8 dB and a little more than that radiated by nine staves. The beamwidth decreases to 10.5°. The on-axis pressure and beamwidth for the corresponding piston are 229.3 dB and 10.9°, respectively.

Consider, next, radiation from array *B* at 9 kHz. The displacement amplitude required for generating omni-directional SL of 220 dB ref. μPa at 1 m is 0.697 μm. The on-axis pressure when 11 of the 32 staves vibrate in-phase with this amplitude is 221.6 dB. The pressure due to phased radiation from 11 of the 32 staves designed to simulate radiation from a piston is shown in Fig. 9. The on-axis pressure is 229.8 dB. It is seen that the

Table 2
Displacements and on-axis pressures for the arrays.

Array	*A*	*B*	*B*	*B*
Frequency (kHz)	10.5	9	7.5	6
Displacement (μm) corresponding to 220 dB omni-pressure in azimuth	0.996	0.697	0.916	1.281
On-axis pressure due to phased radiation from sector (dB) with same displacement. Eleven staves are excited	229.8	229.8	229.4	228.7
On-axis pressure due to radiation into half-space from corresponding rectangular piston with same displacement (dB)	229.3	229.5	228.7	227.7

difference between the omni and phased radiation is 9.8 dB. The on-axis pressure radiated by the corresponding rectangular piston is 229.5 dB and is only a little lower than that radiated by the phased sector.

Consider, next, radiation from array *B* at 7.5 kHz. The displacements required for generating omni-directional pressure of 220 dB ref. μPa at 1 m is 0.916 μm. The on-axis pressure when 11 of the 32 staves vibrate in-phase with this amplitude is 221.9 dB. The pressure due to phased radiation from 11 of the 32 staves designed to simulate radiation from a piston is shown in Fig. 10. The on-axis pressure is 229.4 dB and is nearly the same as the corresponding pressure for array *B*. The on-axis pressure radiated by the corresponding rectangular piston is 228.7 dB and is only a little lower than that radiated by the phased sector.

Consider, finally, radiation from array *B* at 6 kHz. The displacement amplitude required for generating omni-directional pressure of 220 dB is 1.281 μm. The on-axis pressure when 11 of the 32 staves vibrate in-phase with this amplitude is 221.3 dB. The pressure due to phased radiation from 11 of the 32 staves designed to simulate radiation from a piston is shown in Fig. 11. The on-axis pressure is 228.7 dB. The on-axis pressure radiated by the corresponding rectangular piston is 227.7 dB and is lower than that radiated by the phased sector.

The displacements required to generate omni-directional pressure of 220 dB are summarized in Table 2. The on-axis pressures due to phased radiation with the same displacements are also shown. It is seen from the results for array *B* that the required displacement is higher at lower frequencies. As noted earlier, the on-axis pressure for the sector is only a little greater than that for the corresponding rectangular piston. This is due to the larger radiating area of the sector.

4. Conclusions

A method is presented to determine the omni-directional and directional far-field pressures radiated by cylindrical arrays of transducers. The transducers vibrate in the direction of the normal to the array surface and the effect of this is included in the model. Numerical results are presented for the array described by Morris operating at 10.5 kHz and another array operating at 9, 7.5, and 6 kHz.

Numerical results are used to show that the displacement on the surface of the array required to generate 220 dB ref. μPa at 1 m in the omni-directional mode is of the order of 1 μm. Therefore, great care should be taken to ensure that there is no gap between the components used to assemble transducers. Stansfield recommends the use of rigid adhesives at all joints [1].

The pressure generated by in-phase radiation of transducers in a sector is also analyzed. Numerical results show that the on-axis SL is about 221 dB when about one-third of the array is radiating and the displacement is equal to that required to generate 220 dB in the omni-directional mode. The maximum, in this case, does not always occur on the axis because the radiating surface is curved. This is in contrast to radiation from a planar piston radiator of any shape where the maximum always occurs on the normal to the plane because all points on the radiator are equidistant from a point at infinity and on the normal.

Phased radiation of the type used in directional transmissions is also analyzed. The amplitude of the displacement remains the same and the phase is controlled to approximately simulate radiation from a rectangular piston. The displacement is along the normal to the curved surface. The assumption that the radiator is in an infinite cylindrical baffle is used and it is, therefore, not necessary to assume that the power is radiated into a half-space. However, it is seen from Table 2 that there is no significant difference between the

on-axis pressure radiated by a cylindrical sector in an infinite cylindrical baffle and a rectangular piston in an infinite rigid planar baffle. This is also seen in Figs. 7–11 where the beamwidth is nearly the same for the two cases and the pressure radiated in the rear sector is very small. The on-axis pressure radiated by the sector is a little greater than that radiated by the piston because of the slightly larger radiating area.

Acknowledgment

The authors thank Director NPOL for providing facilities and encouragement to do the work.

References

[1] D. Stansfield, *Underwater Electroacoustic Transducers*, Bath University Press, 1990.
[2] P.R. Stepanishen, Radiated power and radiation loading of cylindrical surfaces with non-uniform velocity distributions, *Journal of the Acoustical Society of America* 63 (1978) 328–336.
[3] D.D. Ebenezer, P.R. Stepanishen, A wave-vector-time domain technique to determine the transient acoustic radiation loading on cylindrical vibrators in an inviscid fluid with axial flow, *Journal of the Acoustical Society of America* 89 (1) (1991) 39–51.
[4] P.R. Stepanishen, Modal coupling in the vibrations of fluid loaded cylindrical shells, *Journal of the Acoustical Society of America* 71 (1982) 813–823.
[5] P.R. Stepanishen, D.D. Ebenezer, An eigenvector method to determine the transient response of cylindrical shells in a fluid with uniform axial flow, *Journal of the Acoustical Society of America* 89 (1991) 565–573.
[6] C.H. Sherman, Special relationships between the farfield and the radiation impedances of cylinders, *Journal of the Acoustical Society of America* 43 (1968) 1452–1454.
[7] J.E. Greenspon, C.H. Sherman, Mutual radiation impedance and nearfield pressure for pistons on a cylinder, *Journal of the Acoustical Society of America* 36 (1) (1964) 149–153.
[8] T. Yokoyama, T. Asami, K. Mori, T. Nakamura, A. Hasegawa, Consideration of radiation impedance calculation methods for cylindrical array sound source, *Japanese Journal of Applied Physics* 43 (5B) (2004) 3154–3162.
[9] Y.W. Lam, Fluid–structure coupling in underwater sonar arrays with piston type transducers, *Applied Acoustics* 36 (1992) 31–49.
[10] G.W. Benthien, Numerical modeling of array interactions, in: B.F. Hamonic, O.B. Wilson, J.-N. Decarpigny (Eds.), *Proceedings of the International Workshop*, *Power Transducers for Sonics and Ultrasonics*, 1990, pp. 109–124.
[11] D.T. Laird, H. Cohen, Directionality patterns for acoustic radiation from a source on a rigid cylinder, *Journal of the Acoustical Society of America* 24 (1) (1952) 46–49.
[12] R.L. Rolleigh, J.G. Pruitt, R.H. Stokes, Vertical side-lobe suppression in cylindrical arrays, *Journal of the Acoustical Society of America* 61 (2) (1977) 397–402.
[13] D.D. Ebenezer, Effect of cylindrical baffles on directivity pattern and bandwidth of underwater communication transducer arrays, *Proceedings of the Undersea Defence Technology Pacific*, Sydney, Australia, 1998, pp. 174–178.
[14] P.C. George, A. Paulraj, Optimising the active sonar system design, *Defence Science Journal* 35 (1985) 295–311.
[15] M.C. Junger, D. Feit, *Sound, Structures and Their Interaction*, MIT Press, Cambridge, MA, 1972.
[16] R. Morris, Some practical consideration in the design of sandwich transducers and their array, *IEE Proceedings Part F* 131 (3) (1984).